ASSESSMENT OF WEB CRIPPLING DESIGN PROVISIONS FOR APPLICATION TO PROPRIETARY SOLDIER BEAMS

Marina Bock[a], Marios Theofanous[b], Samir Dirar[b] and Paul Raybone[c]

[a] School of Architecture and Built Environment, University of Wolverhampton, Wolverhampton WV1 1LY, UK
e-mail: marina.bock@wlv.ac.uk

[b] Department of Civil Engineering, University of Birmingham, Edgbaston B15 2TT, UK
e-mail: m.theofanous@bham.ac.uk, S.M.O.H.Dirar@bham.ac.uk

[c] Central Engineering Department, Leada Acrow, Walsall WS9 9AX, UK
e-mail: paulraybone@leadaacrow.com

Keywords: Temporary structures; Experimental behaviour; Cold-formed; Web crippling; two-flange loading; proprietary soldier beams

Abstract. *Structures used for temporary works are lightweight so that they are easy to transport, erect and dismantle. Particular care should be taken in their design as local instabilities could arise due to their thin-walled nature. This article presents 12 tests on proprietary soldier beams subjected to two concentrate opposing loads applied simultaneously. The geometry of the proprietary beams feature cold-formed C-shaped sections with web holes connected back to back with internal spacers. In the absence of design rules for application to such members, the experimental results are used in the present investigation to assess the suitability of the provisions for the web crippling design of cold-formed steel members as well as existing design methods from the literature, which account for the effect of perforations in the web. Experimental and predicted resistances are compared and design recommendations are provided.*

1 INTRODUCTION

Soldier beams are often used in construction as temporary structures that were developed to replace former timber-based products that could not cope with the demands of frequent reuse. They are economic backing members suitable for many propping applications such as horizontal and vertical systems supporting façades or bridge components, braces, trusses spanning openings, secondary beams, heavy duty towers and struts, wailing frames and many others [1]. Soldier beams are lightweight cold-formed members made of high grade steel that comprise two C-shaped members (lipped channel sections) connected by internal spacers at regular intervals. Due to their susceptibility to local instabilities, they are often stiffened with transversal steel plates along their length and are provided with transversal end plates which, in addition, facilitate connection to other members. Upon assembly of all components, the soldier beam becomes a straight member with high load capacity and versatility. The webs of

the C-shaped members have a regular pattern of holes that allow components and/or accessories to be attached almost anywhere along the member length. Their high reusability and recyclability, in combination with their strength and lightweight properties, leads to decreases in energy use and CO_2 emissions hence substantial society-wide benefits.

In Europe, the design of temporary works including falsework and tied access scaffolding is covered in the EN 12812 [2] and the EN 12813 [3]. They contain supplementary information to the Structural Eurocode but mostly include generic structural checks that are of very limited applicability. In addition, it is unclear whether these recommendations apply to proprietary or bespoke equipment and rely on the temporary works designer using additional design guides or codes of practice that might not cover the temporary system to be designed. For instance, in the UK, a commonly used code of practice for temporary works design is the BS 5975 [4]. The BS 5975's principle is the traditional Allowable Stress Design (ASD) and the main problem is that it is skewed towards the management and control aspects of temporary structures rather than their structural design.

In the USA, ASCE/SEI 37 [5] specifies minimum design loads and load combinations against which temporary structures need to be designed. In both European and American codes [2, 5] reduced load return periods are assumed for meteorological actions, which leads to smaller design values for such actions compared to those adopted for permanent structures. Although using small return periods in the design of temporary structures seems reasonable, it has been demonstrated to be unsafe [6], especially for wind actions. Other specific design codes for falsework system are available such as the AASHTO standard GSBTW-1-M [7] and the ACI standard 347-04 [8] which cover the design of bridge falsework systems and formwork for concrete construction, respectively.

The significant level of uncertainty associated with temporary structures is not well captured in existing codes arguably due to the lack of understanding of how such structures actually behave. Research has been conducted on the causes of collapse in temporary structures and methods have been proposed to minimise that risk [9]. This research concluded that temporary structure failures occur mainly due to design and operation issues as well as events associated with underestimating the applied loading and emphasis is placed upon the importance of understanding the limitations of the current existing design methods. In a numerical study by Chan et al. [10], a finite element model was developed to analyse the

buckling behaviour of shoring falsework subjected to high axial loads which was later on validated against test data [11,12]. The same authors proposed analysis and design methods that allow for the different loading conditions during the construction phase in modular falsework [13]. Different modular falsework systems were tested and modelled in [14] that were used by subsequent investigations as benchmark tests. Research conducted in Australia examined the material and structural response of the individual components of falsework and assemblies that were utilised to generate data and propose reliable design models [15-17].

Building on the above mentioned studies, it is noteworthy that the structural behavior of temporary structures subjected to concentrated loading has remained unexplored to date. The research presented in this study addresses structural behaviour of proprietary soldier beams subjected to two opposing concentrated loads (web crippling) applied simultaneously. An example of such is shown in Figure 1 which shows an arrangement of backing members propping the concrete deck of a composite bridge.

Figure 1: Parapet support system employing soldier beams. Courtesy of Leada Acrow.

The capacity of proprietary products like the type of soldier beams examined in the present study is determined by extensive physical testing conducted by the trading company. Tests data is subsequently used to developed in-house technical manuals and datasheets declaring the product capacities for a range of loading likely to occur in practice. Commonly, the designer of temporary works determines the loads that the temporary structure is required to carry and chooses an appropriate soldier beam that can withstand them. Codified design equations are rarely used because their suitability for application to proprietary products has never been assessed.

The current web crippling design provisions for cold-formed steel given in EN 1993-1-3 [18], the North American Specification (NAS) [19] and the Australian/New Zealand Standard [20], consist of a series of empirical equations that mainly depend on the location of the load, the arrangement of the transversal load(s) and cross-sectional shape. In the two latter codes [19, 20], four types of loading are differentiated: End-One-Flange (EOF), Interior-One-Flange (IOF), End-Two-Flanges (ETF) and Interior-Two-Flanges. A different designation system is used in [18] though same loading cases are considered. Emphasis is placed herein on the Two-Flanges loading conditions. The existing web crippling design equations for cold-formed steel were built upon substantial experimental and numerical studies conducted since the mid 1940s [21]. More recent research has been undertaken with new emerging alloys available in construction and more advanced methods of analysis [22-41]

The objectives of this article are first to test a series of proprietary soldier beams subjected to two concentrated opposing loads (web crippling), secondly assess the suitability of the current web crippling design provisions given in EN 1993-1-3 [18], the North American Specification (NAS) [19] and the Australian/New Zealand Standard [20] for application to such proprietary soldier beams, third assess existing design procedures from the literature [42-44] and finally propose design recommendations. The novel aspect of this research is that a commercial product currently available in the market is tested under a load condition commonly encountered in temporary works design. The ultimate aim is to explore if temporary works designers could shift from using in-house design procedures towards existing codes.

2 EXPERIMENTAL INVESTIGATION

The behaviour of soldier beams commonly used for temporary structures has been experimentally investigated and is reported in this section. The scope of the experimental programme covered material tests and web crippling tests under the interior-two-flange and end-two-flange loading conditions which were undertaken at the Structures laboratory of the University of Birmingham.

2.1 Description of the specimens

Three proprietary soldier beams of the “Slim-Lite” type were supplied by Leada Acrow for the purpose of this investigation. The beams were taken from the company’s current inventory and have been used in the past in various construction sites. This was evident both from obvious signs of corrosion observed in two of the three beams tested and from some localized

indentations presumably due to localized damage suffered whilst in service. Hence the behaviour of the tested beams is expected to be representative of the behavior of members already in service for several years or even decades, rather than that of members that have not been in service. All soldier beams had a total length of 3.6 m and comprised two lipped channel sections (C-sections) affixed to one another at regular intervals, as shown in Figure 2. The sections had a nominal overall width *B* of 152 mm, a nominal overall height *H* of 170 mm, a lip depth *d* of 25 mm, an internal spacer in the form a U-profile with a height *s* equal to 42 mm and a nominal thickness *t* of 3.2 mm. The measured dimensions of the three soldier beams are given in Table 1. The degree of corrosion was not an investigated parameter of this study and the effect of corrosion on structural response was accounted for by measuring the specimen thickness upon removal of the corrosion via sand milling. Hence despite the nominal thickness of the specimens being the same, the measured one differed significantly as a result of the varying degree of corrosion.

Table 1: Measured geometric dimensions of the tested soldier beams.

Soldier No.	b (mm)	H (mm)	d (mm)	r (mm)	t (mm)	Length (mm)
S1	55.9	169.6	17.2	1.98	3.95	1700
S2	55.3	169.3	17.6	1.47	2.94	1660
S3	56.3	168.8	19.1	1.37	2.73	1640

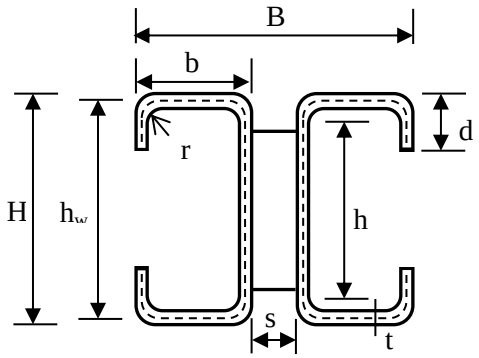

Figure 2: Cross-section of the soldier beam.

The C-sections comprising each soldier beam are connected to one another via four internal spacers in the form of U-profiles. The U-profiles are 3.9 mm thick, have a flange width of 25 mm and a web height of 42 mm. At both ends of the beam, end plates with predrilled holes are welded to the webs of the C-sections to facilitate connection to other members and stiffen the cross-section. Each C-section also has five plate stiffeners welded between the flanges and the web at 600 mm intervals along the length and comprises a pattern of large and small web holes with different diameters located at 300 mm intervals in the spanwise direction. The

diameter d_{wh} of the large web holes is 62 mm whereas the diameter of the small web holes d_{who} is 17 mm. The small web holes are offset 75 mm with respect to the centroid of the large web holes. The arrangement of U-shaped internal spacers, plate stiffeners and holes is illustrated in Figure 3, where half of a typical soldier beam is shown. Several tests were conducted on each soldier beam at various locations along their length with two opposing loads acting simultaneously (web crippling tests), whilst material coupons were also extracted from the same section lengths to determine material properties.

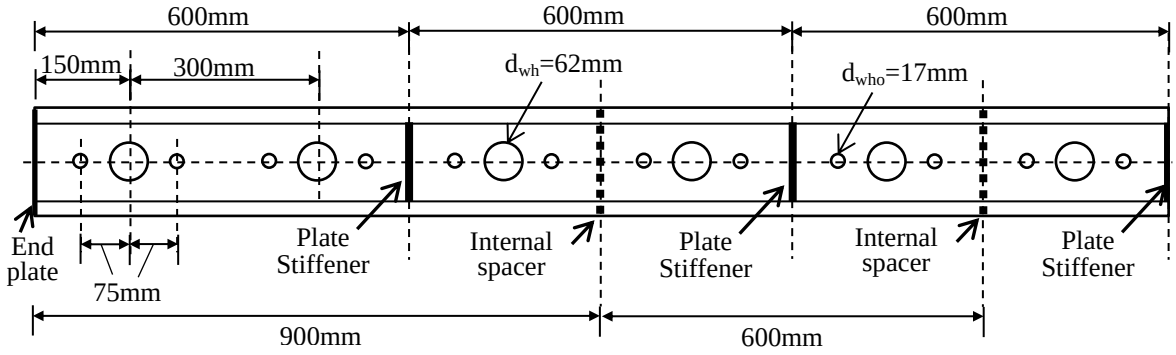

Figure 3: Arrangement of holes, plate stiffeners and internal spacers.

2.2 Material testing

A total of 7 coupon tests were conducted at a static strain rate in accordance with the provisions of EN ISO 6892-1:2016 [45]. The coupons were cut and milled from the flanges of the C-shape members in the longitudinal (rolling) direction. Upon extracting the tensile coupons from the flat parts of the flanges, a small curvature of the coupons was observed due to the release of bending residual stresses. The residual stresses were, however, reintroduced when placing the coupon in the testing machine and are hence implicitly reflected in the obtained stress-strain curve [46]. Prior to testing, the protective paint coating and in some cases a layer of rust were removed from the external surfaces of the coupons. The nominal dimensions of the tensile coupons were 290 mm × 30 mm with the parallel length region having a nominal width of 20 mm. A Vernier digital caliper was used to measure the width and thickness at 3 different locations upon the sample, to the nearest 0.01 mm. A summary of the measured coupon dimensions is presented in Table 2, in which the reported cross-sectional area A_c is based on average values of the measured width and thickness of the coupons taken over three different locations for every coupon, L_c is the parallel length and L_t is the overall length of the coupon. A Zwick 1484 Universal test machine (UTM) was used to load the coupons in tension as shown in Figure 4. An extensometer was attached to measure

the strain and control the loading rate and a data acquisition system was used to record and store the applied load and measured strain at 2 s intervals.

Table 2: Tensile coupon specimen geometry and test results.

Coupon designation	A_c (mm^2)	L_c (mm)	L_t (mm)	E (GPa)	f_{yb} (MPa)	f_u (MPa)	ε_u (%)	ε_f (%)
350-1	75.2	101.59	289	221	360	441	18.2	30.9
350-2	70.9	99.53	290	-*	375	473	17.6	25.6
350-3	77.0	101.57	286	216	343	420	14.5	22.5
450-1	73.3	99.17	289	184	434	495	12.6	19.3
450-2	70.9	99.88	288	211	450	504	12.0	18.3
450-3	67.7	99.44	286	218	442	539	12.1	17.9
450-4	67.2	99.48	286	193	392	503	8.3	13.1

*Young's modulus not logged due to a faulty grip at the beginning of the test

Figure 4: Material coupon testing apparatus and specimen fracture.

The steel used for manufacturing the soldier beams was designated as Grade HA350 to AS 1534 with a minimum yield strength of 350 MPa and a minimum ultimate tensile stress of 430 MPa. The results of the tension coupon tests are graphically shown in a stress-strain diagram in Figure 5. The obtained values for the Young's modulus E, yield strength f_{yb} (0.2 proof stress for coupons not exhibiting yield plateau), ultimate tensile stress f_u and corresponding strain ε_u and strain at fracture ε_f are presented in Table 2. Due to the cold-forming production route of the product, some coupons showed a non-linear material response with minimal yield plateau. Even though the material was specified to a single steel grade, two distinct steel grades with yield strengths approximately equal to 350 MPa and 450 MPa can be identified, hence the coupon designation adopted in Table 2.

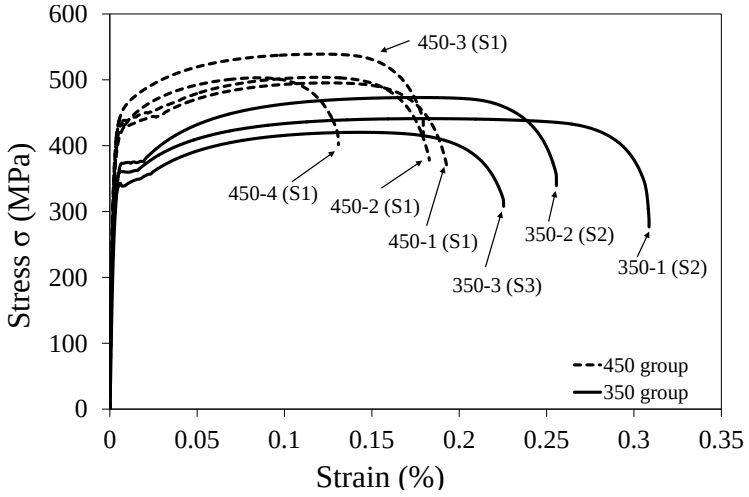

Figure 5: Stress-strain curves for all coupon tensile tests.

2.3 Web crippling tests

The web crippling strength of the soldier beams under two-flange loading condition was investigated by applying a localised transverse load on the top flange directly over a support location. Both load and support reactions were applied by means of 75 mm wide bearing plates. The web crippling strength was determined at four locations along the soldier beam, as shown in Figure 6; at the first hole located 150 mm from the member end, at the second hole located 450 mm from the member end (or 300 mm from the first hole), at the plate stiffener, and at the internal spacer. Each of these four locations has a different overhang length *c* defined as the distance between the edge of the bearing plate and the free end of the soldier beams as shown in Figure 6. Design codes distinguish between interior and end loading conditions according to whether the overhang length c is larger or smaller than $1.5h_w$ (1.5 times the depth of the web) respectively. Figure 7 depicts 3 tests in progress, where the different loading locations can be seen. Moreover, the various degrees of corrosion suffered by the tested specimens can be readily observed, with one specimen appearing in perfect condition and the other two exhibiting clear sings of moderate corrosion.

The bearing resistance of the specimens was determined at the above mentioned four locations for the three soldiers, thus comprising a total of 12 web crippling tests. Due to the loading applied on both flanges simultaneously, the soldiers S1, S2 and S3 are termed TFL1, TFL2 and TFL3, respectively. The ultimate bearing resistance attained at the first hole location $P_{u,h1,test}$, at the second hole location $P_{u,h2,test}$, at the plate stiffener $P_{u,ps,test}$ and at the internal spacer $P_{u,is,test}$ are reported in Table 3. Note that these loads relate to the total applied

load on the specimen, not the load carried by each web. Shortening of the overall height of the beam was being monitored and recorded with two LVDTs placed on either side of the bearing plate loading the top flange. The recorded load – shortening response is shown in Figure 8. Tests were stopped either at extensive deformation beyond ultimate load or upon fracture of the weld between the internal spacer and the C-shape members. Local yielding failure of the web (i.e. web crippling) was achieved in all 12 tests. The response of the specimens when loaded over the 1st or 2nd hole is similar, and is characterised by a gradual loss of stiffness and a smoother post-ultimate response compared to the other tests. Higher carrying capacities were recorded at the internal spacer and at the plate stiffener.

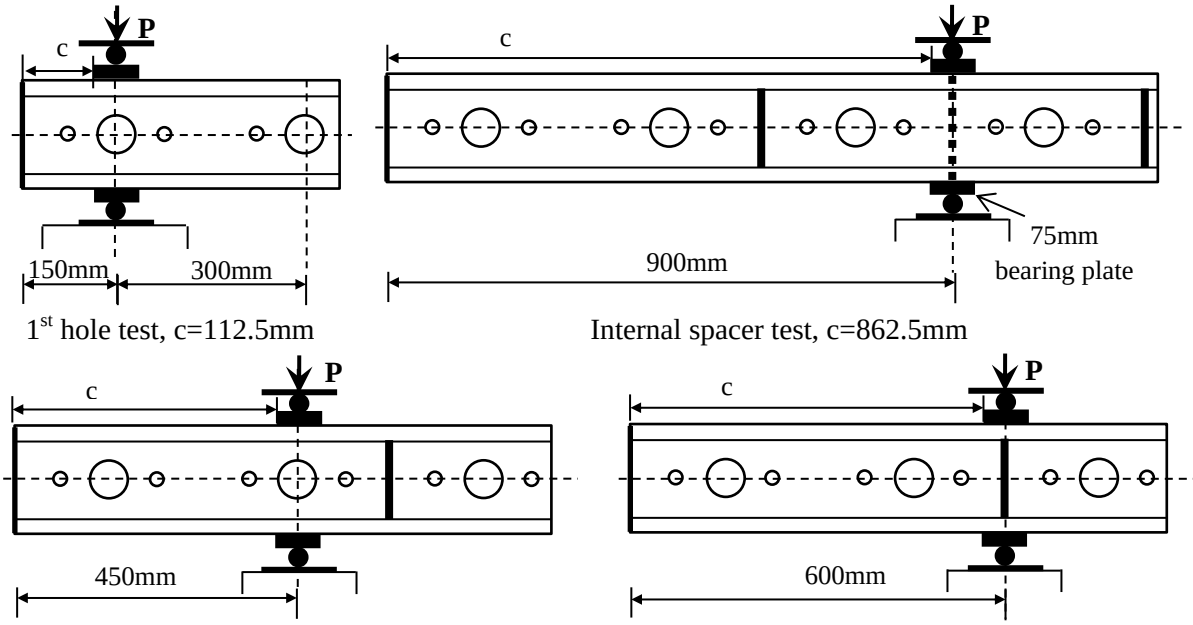

Figure 6: Location of the bearing loads.

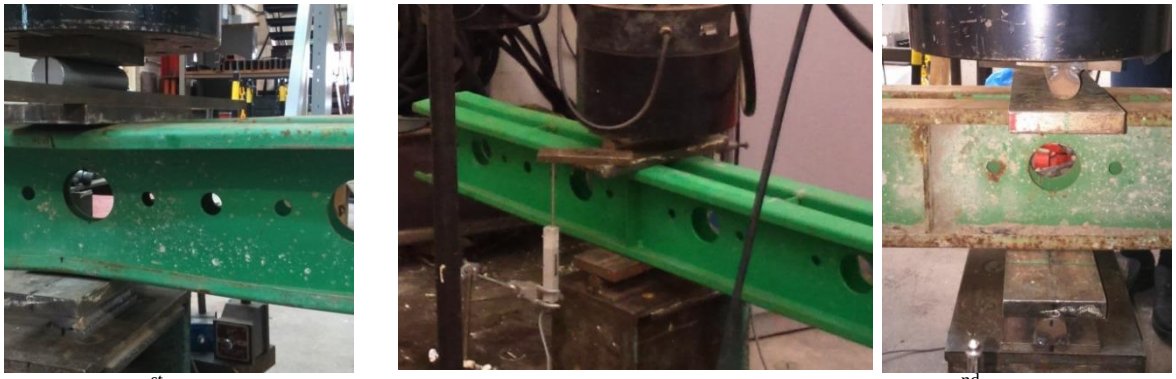

1st hole test | Plate stiffener location test | 2nd hole location test

Figure 7: Test set up for three locations.

Table 3: Total bearing load for all the beams and locations.

Specimen	$P_{u,h1,test}$ (kN)	$P_{u,\ h2,test}$ (kN)	$P_{u,ps,test}$ (kN)	$P_{u,is,test}$ (kN)	$P_{u,\ h2,test}/P_{u,h1,test}$
TFL1	150.1	147	308	240	1.02
TFL2	126	127	328	255	0.99
TFL3	107	122	230	255	0.88

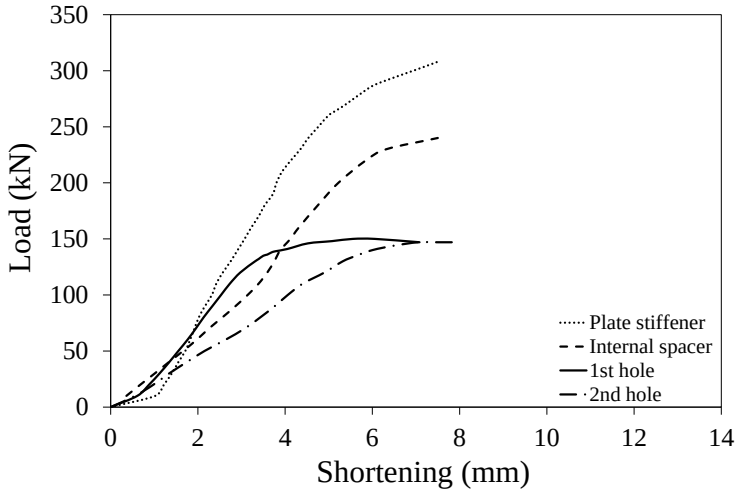

a) TFL1

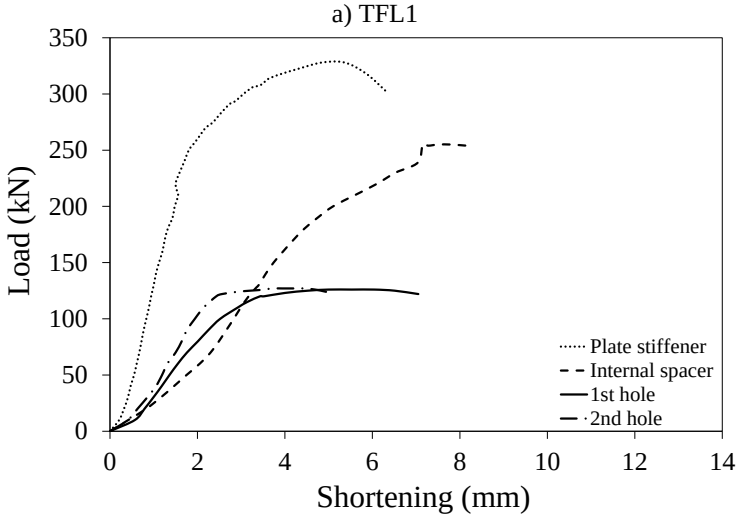

b) TFL2

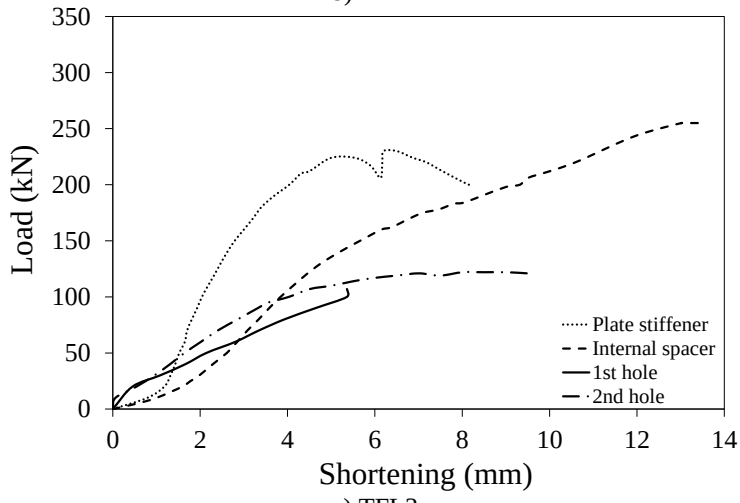

c) TFL3

Figure 8: Load shortening response of tested beams.

3 ASSESSMENT OF DESIGN PROVISIONS FOR WEB CRIPPLING

The experimental data generated in this investigation have been used to assess the ability of existing design equations specified in international design standards to accurately predict the web crippling strength of proprietary soldier beams under two-flange loading condition. The web crippling resistances predicted by EN 1993-1-3 [18], the North American Specification (NAS) [19] and the Australian/New Zealand Standard [20] are being compared against the obtained test results. Existing design methods proposed in the past years based on experimental and numerical studies are also considered in this assessment. These approaches focused on evaluating the influence of web holes on the web crippling strength of cold-formed lipped channel sections [42-44]. Although research into the web crippling response of cold-formed C-sections is available [47-51], the geometries examined in these studies significantly differ from the geometry of the proprietary beams and/or the loading conditions pertinent in the present investigation. The following subsections provide an insight into the current design provisions for web crippling and present the results of the assessment, while an in-depth analysis of the results follows in section 4.

3.1 Design provisions of EN 1993-1-3 [18]

The design provisions covering the resistance to local transverse forces are given in clause 6.1.7 of EN 1993-1-3 [18]. The code differentiates between cross-sections with a single unstiffened or several unstiffened webs, whilst the design of stiffened webs is treated separately. The set of equations specified in clause 6.1.7.2 for application to cross-sections with a single web are compared herein against the experimental resistances previously reported. Depending on the location of the applied load, the following design equations were used to predict the web crippling resistance of the tested sections: Eq. (1) for the 1st hole test and Eq. (2) for the 2nd hole test. Since the code also includes different design equations for application to cross-sections the web rotation of which is restrained, Eq. (3) was used to predict the web crippling strength of the proprietary beams tested at locations with plate stiffener or internal spacer.

$$R_{w,Rd} = k_1 k_2 k_3 \left[6.66 - \frac{h_w/t}{64}\right]\left[1 + 0.01\frac{s_s}{t}\right] t^2 f_{yb}/\gamma_{M1} \qquad \text{if } c \leq 1.5h_w \tag{1}$$

$$R_{w,Rd} = k_3 k_4 k_5 \left[21 - \frac{h_w/t}{16.3}\right]\left[1 + 0.0013\frac{s_s}{t}\right] t^2 f_{yb}/\gamma_{M1} \qquad \text{if } c > 1.5h_w \tag{2}$$

$$R_{w,Rd} = k_8 k_9 \left[13.2 + 2.87\sqrt{\frac{s_s}{t}}\right] t^2 f_{yb}/\gamma_{M1} \qquad \text{if } c > 1.5h_w \tag{3}$$

In the aforementioned equations, $R_{w,Rd}$ is the local transverse resistance of one web, h_w is the web height between the midlines of the flanges, t is the cross-sectional thickness, s_s is the length of the bearing plate, f_{yb} is the material yield strength in MPa, γ_{M1} is a partial safety set to unity and k_i are dimensionless coefficients given by Eqs. (4)-(10) where r is the internal radius of the corners, ϕ is the angle of the web relative to the flanges in degrees and $k=f_{yb}/228$.

$$k_1 = 1.33 - 0.33/k \quad (4)$$

$$k_2 = 1.15 - 0.15r/t \text{ but } k_2 \geq 0.5 \text{ and } k_2 \leq 1 \quad (5)$$

$$k_3 = 0.7 + 0.3(\phi/90)^2 \quad (6)$$

$$k_4 = 1.22 - 0.22k \quad (7)$$

$$k_5 = 1.06 - 0.06r/t \text{ but } k_5 \leq 1 \quad (8)$$

$$k_8 = 1/k \text{ if } s_s/t < 66.5;\ k_8 = (1.1 - h_w/(665t))/k \text{ if } s_s/t > 66.5 \quad (9)$$

$$k_9 = 0.82 + 0.15t/1.9 \quad (10)$$

The design predictions for each of the locations subjected to two-flange loading are designated as $P_{u,h1,EC3}$, $P_{u,h2,EC3}$, $P_{u,ps,EC3}$ and $P_{u,is,EC3}$ for loads applied at the 1st hole, 2nd hole, plate stiffener and internal u-shaped spacer respectively. The resulting design strengths are reported in Table 4 where the mean value and the coefficient of variation of the experimental over predicted web crippling resistances are also reported. Figure 9 shows the test-to-predicted strength ratio $P_{u,test}/P_{u,EN\ 1993\text{-}1\text{-}3}$ plotted against the web slenderness of the soldier beam defined as the web height to thickness ratio h_w/t. The h_w/t ratios of each beam are 41.93 for TFL1, 56.59 for TFL2 and 60.83 for TFL3.

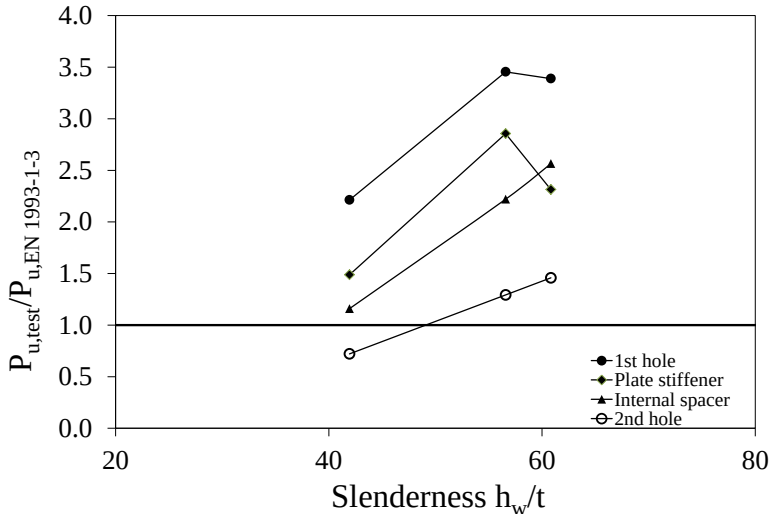

Figure 9: Assessment of the EN 1993-1-3 for the four test locations

Table 4: Assessment of the EN 1993-1-3 design provisions based on a test-to-predicted ratio

Specimen	$P_{u,h1,test}/P_{u,h1,EC3}$	$P_{u,h2,test}/P_{u,h2,EC3}$	$P_{u,ps,test}/P_{u,ps,EC3}$	$P_{u,is,test}/P_{u,is,EC3}$
TFL1	2.21	0.72	1.49	1.16
TFL2	3.45	1.29	2.86	2.22
TFL3	3.39	1.46	2.31	2.57
Mean	3.02	1.16	2.22	1.98
COV	0.189	0.273	0.253	0.302

3.2 Design provisions of the North American Specification (NAS) [19] and the Australian/New Zealand Standard [20].

The provisions for the web crippling resistance are given in clause C3.4 of the NAS [19] and clause 3.3.6 of the Australian/New Zealand Standard [20]. Both codes specify identical design equations for the determination of the web crippling resistance, albeit using different symbols to refer to the same parameters. Unlike EN 1993-1-3 [18] where a set of equations is presented, The NAS [19] and the Australian/New Zealand Standard [20] use the unified expression given by Eq. (11), which is applicable to cross-sections without holes. A reduction factor is to be used to account for the presence of a web hole under the bearing load. It is noteworthy that the presence of holes is currently not accounted for in EN 1993-1-3 [18].

The previously adopted notation for the EN 1993-1-3 is used to symbolize the relevant parameters in Eq. (11). Note that, however, Eq. (11) uses the flat part of the web h instead of the distance between midlines of the flanges h_w, as is the case for EN 1993-1-3; both h_w and h are defined in Figure 1. This unified equation also includes four dimensionless coefficients which depend on the cross-section geometry, load condition, and support and flange conditions: C, C_r, C_s and C_h. Based on the tests reported herein, the values for these coefficients were determined assuming unfastened support conditions, unstiffened flanges and two-flange loading condition. Similar to the provisions of EN 1993-1-3 and considering the overhang length c of each test, the test at the location of the 1st hole was identified as end loading condition (i.e. c<1.5h) while the tests at the location of the 2nd hole, the plate stiffener and the internal spacer were identified as interior loading condition (i.e. when c>1.5h). Regarding cross-section geometry, the coefficients for built-up sections and single web channel and C-sections given in tables C3.4.1-1 and C3.4.1-2 of the NAS [19] were used for comparison purposes. The same coefficients are given in tables 3.3.6.2(A) and 3.3.6.2(B), respectively, in the Australian/New Zealand Standard [20]. The geometry and loading arrangement of the tested soldier beams are within the limits of applicability of Eq. (11).

$$R_{w,Rd} = Ct^2 f_{yb} \sin\phi \left(1 - C_r\sqrt{r/t}\right)\left(1 + C_s\sqrt{s_s/t}\right)\left(1 - C_h\sqrt{h/t}\right) \quad (11)$$

The existence of a web hole within the bearing length s_s, as is the case in this experimental investigation, is accounted for through a reduction factor R_c. Again, based on the overhang length *c*, Eqs. (12) or (13), where *x* is the nearest distance between the web hole and nearest bearing length, should be used. Eqs. (12) and (13) are applicable as long as (i) webs are under one flange loading condition, (ii) clear distance between holes is greater than 457 mm and (iii) the distance of the holes for the beam end is at least equal to the web depth h. Clearly none of these conditions is met by the tested specimens, but, in the absence of alternative means to account for the effect of the holes, the applicability of Eqs. (12) and (13) is assessed herein.

$$R_c = 1.01 - 0.325\, d_{wh}/h + 0.083\, x/h \qquad \text{if } c \le 1.5h \quad (12)$$

$$R_c = 0.90 - 0.047\, d_{wh}/h + 0.053\, x/h \qquad \text{if } c > 1.5h \quad (13)$$

The design predictions for each of the locations subjected to two-flange loading are designated as $P_{u,h1,A/A/NZ}$, $P_{u,h2,A/A/NZ}$, $P_{u,ps,A/A/NZ}$ and $P_{u,is,A/A/NZ}$ for loads applied at the 1st hole, 2nd hole, plate stiffener and internal u-shaped spacer. The resulting design predictions are reported in Table 5 for the assessment of the code when coefficients for built-up sections are used, whilst Table 6 presents the results for the assessment of the code when coefficients for single web channel sections and C-sections are used. The tables show in brackets the reduced web crippling strength upon applying the reduction factor R_c to account for the effect of the web holes on the design resistance. A graphical comparison between experimental and codified web crippling resistances is presented in Figures 10 and 11 for loading at the location of stiffeners and of holes respectively.

Table 5: Assessment of the NAS and the Australian/New Zealand Standard using coefficients for built-up sections based the test-to-predicted ratio.

Specimen	$P_{u,h1,test}/P_{u,h1,A/A/NZ}$	$P_{u,h2,test}/P_{u,h2,A/A/NZ}$	$P_{u,ps,test}/P_{u,ps,A/A/NZ}$	$P_{u,is,test}/P_{u,is,A/A/NZ}$
TFL1	0.77 (0.87)*	0.34 (0.38)*	0.70	0.55
TFL2	1.41 (1.60)*	0.64 (0.72)*	1.65	1.28
TFL3	1.40 (1.58)*	0.71 (0.81)*	1.35	1.49
Mean	1.19 (1.35)*	0.56 (0.64)*	1.23	1.11
COV	0.253 (0.252)*	0.290 (0.290)*	0.319	0.365

* Reduced values to allow for hole under bearing load

Table 6: Assessment of the NAS and the Australian/New Zealand Standard using coefficients for single web channel and C-sections based the test-to-predicted ratio.

Specimen	$P_{u,h1,test}/P_{u,h1,A/A/NZ}$	$P_{u,h2,test}/P_{u,h2,A/A/NZ}$	$P_{u,ps,test}/P_{u,ps,A/A/NZ}$	$P_{u,is,test}/P_{u,is,A/A/NZ}$
TFL1	1.22 (1.39)*	0.44 (0.50)*	0.92	0.72
TFL2	2.29 (2.58)*	0.77 (0.88)*	1.99	1.55
TFL3	2.27 (2.57)*	0.85 (0.96)*	1.60	1.77
Mean	1.93 (2.18)*	0.69 (0.78)*	1.50	1.35
COV	0.258 (0.257)*	0.258 (0.258)*	0.294	0.337

* Reduced values to allow for hole under bearing load

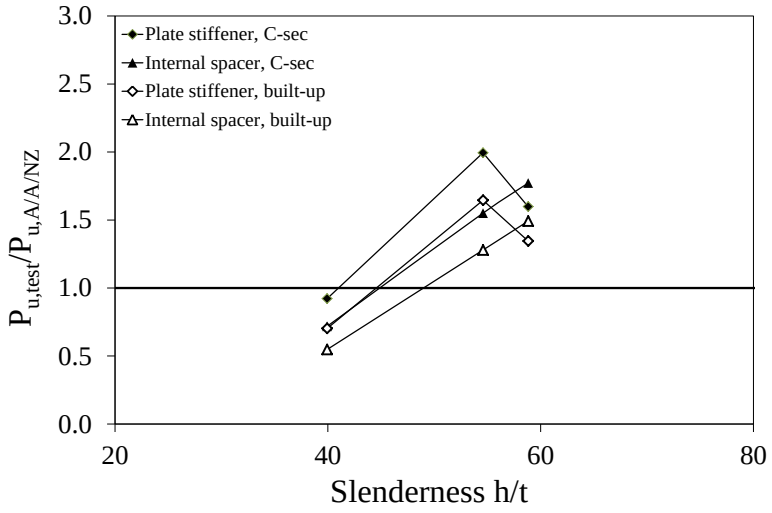

Figure 10: Assessment of NAS and the Australian/New Zealand Standard at locations without holes

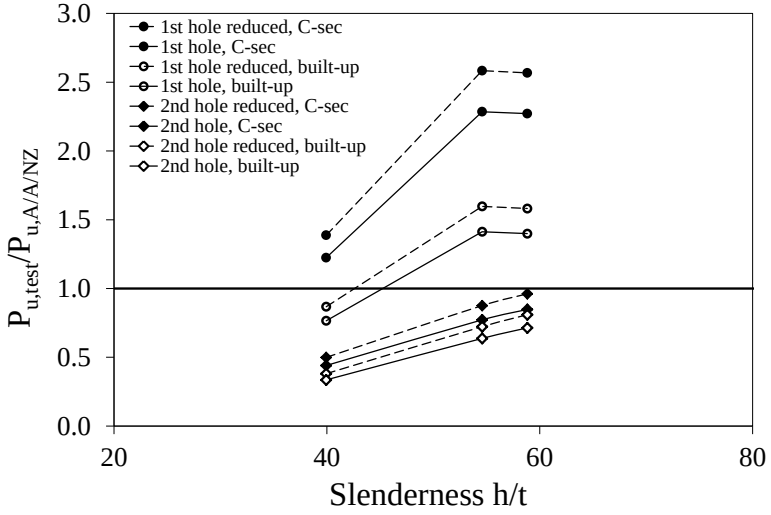

Figure 11: Assessment of NAS and the Australian/New Zealand Standard at locations with web holes.

3.3 Design recommendations by Uzzaman et al. [40-42]

Uzzaman et al. conducted a series of experimental and numerical studies on the web crippling strength of cold-formed steel channel sections with centred web holes under bearing loads [44, 51] and with offset web holes [42, 43] under interior and end-two-flange loading conditions. Following a regression analysis, they proposed the adoption of the reduction factors R_c defined by Eqs. (14) and (15) for the web crippling strength of webs with centred holes and Eqs. (16) and (17) for the web crippling strength of webs with offset holes as a means to account for the effect of web holes on the web crippling strength. Given their empirical nature, these equations are only valid for cross-sections with web holes meeting certain geometric limitations, namely $h/t \leq 159$, $s_s/t \leq 84$, $s_s/h \leq 63$, $d_{wh}/h < 0.8$ and $\phi = 90°$. The specimens tested in the present study meet these limitations, hence the equations recommended by Uzzaman et al. [42-44] are well-suited to predict the effect of web holes on the web crippling strength.

For webs with holes under bearing length:

$$R_{c,centred} = 0.90 - 0.6\, d_{wh}/h + 0.12\, s_s/h \leq 1 \qquad \text{if } c \leq 1.5h \qquad (14)$$

$$R_{c,centred} = 1.05 - 0.54\, d_{wh}/h + 0.01\, s_s/h \leq 1 \qquad \text{if } c > 1.5h \qquad (15)$$

For webs with offset holes:

$$R_{c,offset} = 0.95 - 0.49\, d_{wh}/h + 0.17\, x/h \qquad \text{if } c \leq 1.5h \qquad (16)$$

$$R_{c,offset} = 1.00 - 0.45\, d_{wh}/h + 0.09\, x/h \qquad \text{if } c > 1.5h \qquad (17)$$

In this assessment, the reduction factors proposed by Uzzaman et al. [42-44] have been used to reduce the web crippling resistance predicted by EN 1993-1-3, the NAS and the Australian/New Zealand Standard to account for the web holes present in the soldier beams. Since the soldier beams have both centred and offset holes, two cases have been considered: (1) accounting only for the effect of the large centred web hole on the web crippling resistance (i.e. $R_{w,Rd} \times R_{c,centred}$) and (2) accounting for the effect of both the centred larger hole and the offset smaller holes on the web crippling strength (i.e. $R_{w,Rd} \times R_{c,centred} \times R_{c,offset}$). The results of the assessment are presented in Tables 7 to 9, whilst a graphical representation is provided in Figures 12-14. Note that in these figures the legend shows a number between brackets correlating the displayed data with the case under consideration.

Table 7: Assessment of the reduced web crippling resistance predicted by EN 1993-1-3 using reduction factors proposed by Uzzaman et al.

Specimen	$R_{w,Rd} \times R_{c,centred}$		$R_{w,Rd} \times R_{c,centred} \times R_{c,offset}$	
	$P_{u,h1,test}/P_{u,h1,EC3}$	$P_{u,h2,test}/P_{u,h2,EC3}$	$P_{u,h1,test}/P_{u,h1,EC3}$	$P_{u,h2,test}/P_{u,h2,EC3}$
TFL1	2.48	0.86	2.67	0.88
TFL2	3.55	1.53	3.82	1.58
TFL3	3.40	1.72	3.66	1.78
Mean	3.14	1.37	3.38	1.41
COV	0.150	0.271	0.150	0.271

Table 8: Assessment of the reduced web crippling resistance predicted by the NAS and the Australian/New Zealand Standard using reduction factors proposed by Uzzaman et al. and coefficients for built-up sections

Specimen	$R_{w,Rd} \times R_{c,centred}$		$R_{w,Rd} \times R_{c,centred} \times R_{c,offset}$	
	$P_{u,h1,test}/P_{u,h1,A/A/NZ}$	$P_{u,h2,test}/P_{u,h2,A/A/NZ}$	$P_{u,h1,test}/P_{u,h1,A/A/NZ}$	$P_{u,h2,test}/P_{u,h2,A/A/NZ}$
TFL1	0.86	0.40	0.92	0.41
TFL2	1.45	0.75	1.56	0.78
TFL3	1.40	0.84	1.51	0.87
Mean	1.24	0.67	1.33	0.69
COV	0.217	0.289	0.217	0.289

Table 9: Assessment of the reduced web crippling resistance predicted by the NAS and the Australian/New Zealand Standard using reduction factors proposed by Uzzaman et al. and coefficients for single web channel and C-sections

Specimen	$R_{w,Rd} \times R_{c,centred}$		$R_{w,Rd} \times R_{c,centred} \times R_{c,offset}$	
	$P_{u,h1,test}/P_{u,h1,A/A/NZ}$	$P_{u,h2,test}/P_{u,h2,A/A/NZ}$	$P_{u,h1,test}/P_{u,h1,A/A/NZ}$	$P_{u,h2,test}/P_{u,h2,A/A/NZ}$
TFL1	1.37	0.52	1.48	0.54
TFL2	2.35	0.91	2.53	0.94
TFL3	2.28	1.00	2.45	1.03
Mean	2.00	0.81	2.15	0.84
COV	0.222	0.256	0.222	0.256

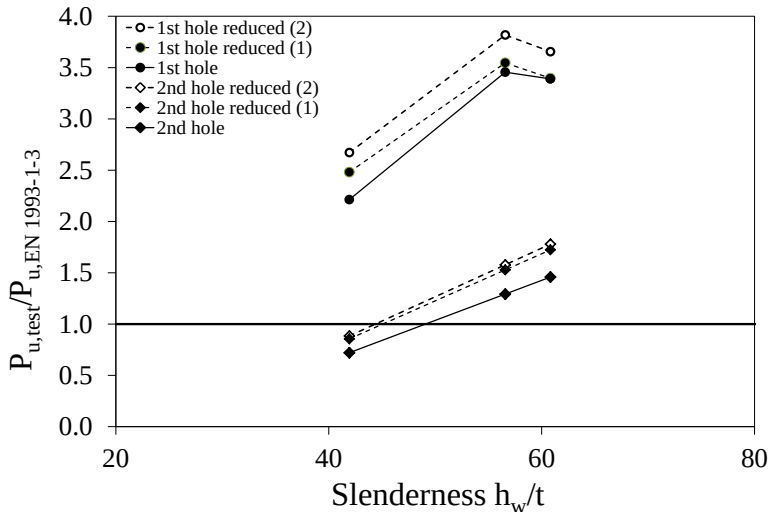

Figure 12: Reduced test-to-predicted ratio by EN 1993-1-3 using Uzzaman et al. reduction factors

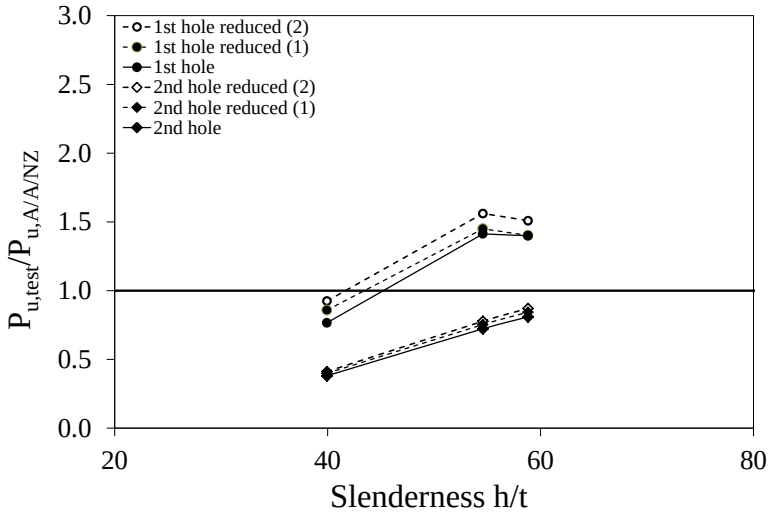

Figure 13: Reduced test-to-predicted ratio by the NAS and the Australian/New Zealand Standard using Uzzaman et al. reduction factors and coefficients for built-up sections

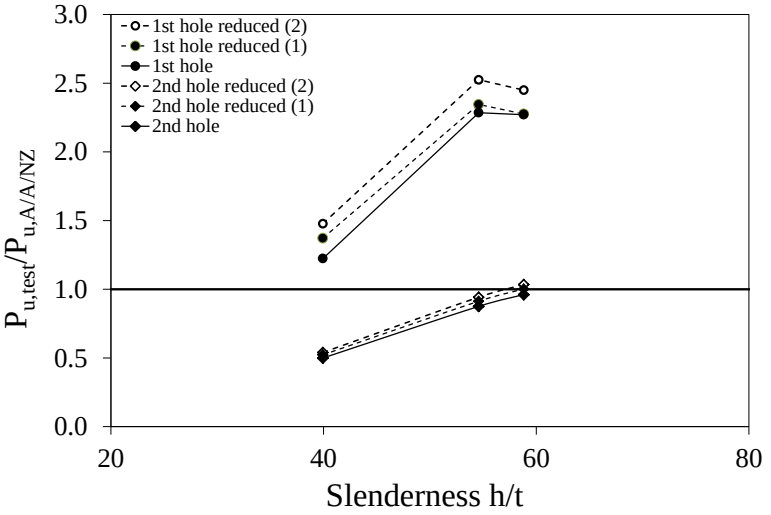

Figure 14: Reduced test-to-predicted ratio by the NAS and the Australian/New Zealand Standard using Uzzaman et al. reduction factors and coefficients for single web channel and C-sections

4 DISCUSSION AND DESIGN RECOMMENDATIONS

Among the three design standards considered, EN 1993-1-3 [18] is the most conservative one, as it results in the highest test-to-predicted strength ratios. With the exception of the predicted web crippling strength over the location of the 2nd hole of the stockiest soldier beam, all of the web crippling resistances predicted by EN 1993-1-3 [18] are on the safe side (i.e. $P_{u,test}/P_{u,EN,1993\text{-}1\text{-}3}$ ratio > 1). Moreover, as shown in Fig. 9, the design predictions become increasingly conservative with increasing web slenderness, thus revealing that the codified design equations do not properly account for the effect of web slenderness. The COV values, ranging from 0.189 to 0.302, are the lowest among all design standards as a consequence of a high test-to-predicted strength mean values.

The design predictions of the NAS [19] and the Australian/New Zealand Standard [20] are unduly conservative for end-two-flange loading when the web slenderness is over 50, whilst they become unsafe for low slenderness values. The test-to-predicted ratios are lower when dimensionless coefficients for built-up sections are used thereby showing that those standards expect built-up sections to have better web crippling performance than single web sections of C-shaped section. Both NAS [19] and the Australian/New Zealand Standard [20] show overly high COV ranging from 0.252 to 0.365, likewise EN 1993-1-3, which again reflects that the formulae do not capture accurately the influence of the web slenderness.

Both the NAS [19] and the Australian/New Zealand Standard [20] are safe when used to predict the web crippling strength at locations where there are no holes (i.e. internal stiffener and u-shape spacer), albeit unsafe for stockier webs. At the first hole, the design predictions are safe regardless of the dimensionless coefficients used with the exception of the predicted web crippling strength of the stockiest soldier beam when coefficients for built-up sections are used. At the second hole, the design predictions are always unsafe. Accounting for web holes through a reduction factor applied to the predicted web crippling strength, results in lower predictions and consequently higher test-to-predicted ratios. Overall, in the presence of a hole a decrease of about 10-15% in the web crippling strength is predicted by the NAS and the Australian/New Zealand Standard leading to even more conservative predictions at the first hole and yet unsafe predictions at the second hole.

The web crippling design resistances predicted by EN 1993-1-3 [18], the NAS [19] and the Australian/New Zealand Standard [20] were reduced considering two approaches to Uzzaman's et al. [42-44] reduction factors. Overall, it is observed that the reduction factors are smaller with increasing distance between the bearing load and the free end.

The results show that the EN 1993-1-3 [18] test-to-predicted ratios upon applying Uzzaman's et al. [42-44] reduction factors at the 1st hole location become even more conservative. Again, the predicted web crippling strength over the 2nd hole location for the stockiest soldier beam appears as the only unsafe value. However, its reduced web crippling resistance is underestimated by 12% as opposed to the original underestimation which was 28%.

Regarding the NAS [18] and the Australian/New Zealand Standard [19] predictions upon applying Uzzaman's et al. [42-44] reduction factors, at the 1st hole location it is observed slightly less scatter and improved predictions. For the stockiest proprietary beam, this method is not adequate when using dimensionless coefficients for built-up sections likewise reducing the web crippling strength with the current formulae of the standards. The use of Uzzaman's et al. [42-44] equations to reduce the web crippling strength of the proprietary soldier beam at the 2nd hole location, improves the mean test-to predicted strength value but predictions lay mostly on the unsafe side. Thus, further investigation is required to accurately understand the web crippling response at this location corresponding to the interior two-flange condition.

Following the above-mentioned discussion of the various assessments carried out, the following design recommendations are given for proprietary soldier beams with web holes subjected to web crippling under the two-flange loading condition:

- EN 1993-1-3 is safe to predict the web crippling strength for end-two-flange loading as well as for interior-two-flange loading at the plate stiffener and the internal spacer.
- For interior two-flange loading at the hole location, EN 1993-1-3 is safe for application to proprietary beams with web slenderness h_w/t greater or equal to 56 but unsafe for low web slenderness values.
- In the presence of web holes, it is recommended not to account for any reduction coefficient to reduce the web crippling strength as that would lead to overly conservative predictions.
- Reducing the EN 1993-1-3 web crippling predictions through Uzaaman's et al. reduction factor to account for web holes interior loading conditions improves unsafe predictions in proprietary beams with web slenderness h_w/t value of 41.93.
- The web crippling design equations in the NAS and the Australian/New Zealand Standard are the same and both are safe to predict the web crippling strength at locations without holes in proprietary beams with slenderness ratios h/t greater or equal to 54. Either dimensionless coefficients for built-up sections or single web sections or C-sections were observed to be adequate.
- For lower slenderness (i.e. h/t value of 39.93), those standards are not adequate.
- At the 1st hole location, it is recommended to use the dimensionless coefficients for single web sections or C-sections but not to reduce the web crippling strength to account for web holes using the current codified equation as that would lead to overly conservative

predictions. Moreover, the examined geometries and cross-section do not meet the limits of application of the current reduction factor.

- The reduction factors proposed by Uzzaman et al. are safe to predict the reduced web crippling strength accounting for web holes at the 1st hole location regardless the dimensionless coefficients used for specimens with high slenderness (i.e h/t values greater than 54.59).
- At the 1st hole, the most efficient design is achieved when coefficients for built-ups are used to determine the web crippling strength and subsequently reduced by multiplying Uzzaman's et al reduction factor for centred holes and Uzzaman's et al reduction factor for offset holes.
- It is not recommended to use the NAS and the Australian/New Zealand Standard at the 2nd hole location. It is noteworthy, however, that applying the reduction factor for centred holes multiplied by the reduction factor for offset holes proposed by Uzzaman's et al. improves over predictions and almost shift the predictions to the safe side.

5 CONCLUSIONS

A series of tests on proprietary soldier beams were conducted to obtain their structural behavior and web crippling strength under two-flange loading condition. Both end and interior two-flange loading have been considered. All specimens were representative of currently-in-service proprietary soldier beams and comprised lipped C-sections with patterns of web holes at regular intervals. Material coupon tests were also conducted to obtain the material response and were reported herein. In the absence of available methods the suitability of the web crippling design provisions given in international design standards for the design of cold-formed steel structures including the EN 1993-1-3 [18], the NAS [19] and the Australian/New Zealand Standard [20] were assessed. Two sets of dimensionless coefficients were considered in the assessment of the two latter design provisions [19, 20]. It was found that these standards significantly underestimate the web crippling strength for high web-slenderness values, particularly under end loading conditions. On the contrary, with decreasing slenderness the predictions were found to lie on the unsafe side for interior two-flange loading. In most cases a very high scatter of the design predictions was observed, arguably due to the effect of the web-slenderness that was found to strongly affect the predicted design strengths.

Design equations that explicitly allow for the effect of holes in the web on the web crippling strength [42-44] were applied in conjunction with all three design standards and were found to reduce the scatter in the predictions. However, the improvements were marginal as the underlying reason for poor agreement between experimental results and design predictions seems to be the base equations specified for interior two-flange loading. Further research is needed to better capture the effect of the distance of the point of load application from the beam end to define a more accurate boundary between interior and end loading conditions. In addition to this and since it has not been within the scope of the present paper but can be observed in practical uses of soldier beams, further research is also suggested on soldier beams subjected to one-flange loading conditions.

ACKNOWLEDGEMENTS

The authors would like to acknowledge Leada Acrow for the donation of the specimens and funding received under the grant ID UoB-RA-14-0342 which has led to the research presented in this publication.

REFERENCES

[1] Leada Acrow Slim-Lite Soldier System. General Technical and Application Manual. Formwork product Technical Guide, Slough, 2018.

[2] EN 12812:2008. Falsework — Performance requirements and general design. CEN European Committee for Standarization, 2008.

[3] EN 12813:2004. Temporary works equipment - Load bearing towers of prefabricated components - Particular methods of structural design. CEN European Committee for Standarization, 2004.

[4] BS 5975:1982 – Code of practice for falsework (1st ed.). London, UK: British Standards Institution (BSI), 1982.

[5] ASCE/SEI 37–14 – Design loads on structures during construction. American Society of Civil Engineers (ASCE), 2014.

[6] Sexsmith RG and Reid SG, Safety factors for bridge falsework by risk management. Structural Safety, 25(2), 227–243 (2003).

[7] AASHTO GSBTW–1–M – Guide design specifications for bridge temporary works, with 2008 interim revisions (1st ed.). Washington, DC: American Association of State Highway and Transportation Officials (AASHTO), 2008.

[8] ACI 347–04 – Guide to formwork for concrete. Washington, DC: American Concrete Institute (ACI), 2004.

[9] Beale R. and João A. Design Solutions and Innovations in Temporary Structures. IGI Global, Hershey PA, USA, 2017.

[10] Chan S, Zhou Z, Chen W, Peng J and Pan A, Stability analysis of semi-rigid steel scaffolding, Engineering Structures, 17(8), 568–574, 1995.

[11] Peng J, Pan A, Rosowsky D, Chen W, Yen T and Chan S, High clearance scaffold systems during construction - I. Structural modelling and modes of failure, Engineering Structures, 18(3), 247–257, 1996.

[12] Peng J, Pan A, Rosowsky D, Chen W, Yen T and Chan S, High clearance scaffold systems during construction - II. Structural analysis and development of design guidelines, Engineering Structures, 18(3), 258–267, 1996.

[13] Peng J, Pan A and Chan S, Simplified models for analysis and design of modular falsework, Journal of Constructional Steel Research, 48(2–3), 189–209, 1998.

[14] Weesner L and Jones H, Experimental and analytical capacity of frame scaffolding, Engineering Structures, 23(6), 592–599, 2001.

[15] Chandrangsu T and Rasmussen K, Investigation of geometric imperfections and joint stiffness of support scaffold systems, Journal of Constructional Steel Research, 67(4), 576–584, 2011.

[16] Chandrangsu T and Rasmussen K, Structural modelling of support scaffold systems, Journal of Constructional Steel Research, 67(5), 866–875, 2011.

[17] Zhang H, Chandrangsu T and Rasmussen K, Probabilistic study of the strength of steel scaffold systems, Structural Safety, 32(6), 393–401, 2010.

[18] EN 1993-1-3. Eurocode 3 – Design of Steel Structures – Part 1-3: General rules – Supplementary rules for cold-formed members and sheeting. European Committee for standardization.

[19] NAS. North American Specification for the Design of Cold-Formed Steel Structural Members, AISI ANSI S100-16, American Iron and Steel Institute, Washington, D.C, 2016.

[20] Australian/New Zealand Standard (AS/NZS), Cold-Formed Steel Structures, AS/NZS 4600:2018, Standards Australia, Sydney, Australia, 2005.

[21] Winter G and Pian RHJ. Crushing strength of thin steel webs. Engineering experiment station,

Bulletin No. 35, Part 1. New York, USA; 1946.

[22] Bakker MCM, Stark JWB, Theoretical and experimental research on web crippling of cold-formed flexural steel members. Thin-Walled Structures, 18, 261-90, 1994.

[23] Hofmeyer H, Kerstens JGM, Snijder HH, Bakker MCM, New prediction model for failure of steel sheeting subject to concentrated load (web crippling) and bending. Thin-Walled Structures, 39, 773-96, 2001.

[24] Duarte APC and Silvestre N, A new slenderness-based approach for the web crippling design of plain channel steel beams. International Journal of Steel Structures, 3, 421-34, 2013.

[25] Young B and Hancock GJ, Design of cold- formed channels subjected to web crippling. Journal of Structural Engineering, 127, 1137-44, 2001.

[26] Zhao XL and Hancock GJ, Square and rectangular hollow sections subjected to combined actions. Journal of Structural Engineering, 118, 648-68, 1992.

[27] Zhao XL and Hancock GJ, Square and rectangular hollow sections under transverse end-bearing force. Journal of Structural Engineering, 121, 1323-9, 1995.

[28] Zhou F and Young B. Yield line mechanism analysis on web crippling of cold-formed stainless steel tubular sections under two-flange loading. Engineering Structures , 28, 880-92, 2006.

[29] Bock M, Real E, Mirada FX, Statistical evaluation of a new resistance model for cold-formed stainless steel cross-sections subjected to web crippling. International Journal of steel structures, 15(1), 227-244, 2015.

[30] Dos Santos GB, Gardner L, Kucukler M, A method for the numerical derivation of plastic collapse loads. Thin-Walled Structures, 124, 258-277, 2018.

[31] Li H-T and Young B. Tests of cold-formed high strength steel tubular sections undergoing web crippling. Engineering Structures, 141, 571-583, 2017.

[32] Young B and Hancock GJ. Web crippling behavior of cold-formed unlipped channels. In: Proceedings of the 14th International specialty conference on cold-formed steel structures; 1998 October; Missouri, U.S.A; 1998.

[33] Beshara B, Schuster M. Web crippling data and calibrations of cold-formed steel members. AISI Research Report RP00-2. 2000 American Iron and Steel Institute; Washington, DC.

[34] Zhou F, Young B. Experimental investigation of cold-formed high-strength stainless steel tubular members subjected to combined bending and web crippling. Journal of Structural Engineering (ASCE) 2007;133:1027–34.

[35] Gardner L, Talja A, Baddoo NR, Structural design of high-strength austenitic stainless. Thin-Walled Structures, 44, 517–28, 2006.

[36] Bock M, Real E, Strength curves for web crippling design of cold-formed stainless steel hat sections. Thin-Walled Structures, 85, pp. 93-105, 2014.

[37] Yousefi AM, Lim JBP and Clifton GC, Web bearing capacity of unlipped cold-formed ferritic stainless steel channels with perforated web subject to end-two-flange (ETF) loading. Engineering Structures, 152, pp. 804-818, 2017.

[38] Gunalan S and M Mahendran M, Web crippling tests of cold-formed steel channels under two flange load cases. Journal of Constructional Steel Research., 110, pp. 1-15, 2015.

[39] Yousefi AM, Uzzaman A, Lim JBP, Clifton GC, Young B, Web crippling strength of cold-formed stainless-steel lipped channels with web perforations under end-two-flange loading. Advances in Structural Engineering, 20(12), 1845-1863, 2017.

[40] Sundararajah L, Mahendran M and Keerthan P, Experimental studies of lipped channel beams subject to web crippling under two-flange load cases. Journal of Structural Engineering, 142(9):04016058, 2016.

[41] Nguyen VV, Hancock GJ, Pham CH, New developments in the Direct Strength Method (DSM) for design of cold- formed steel sections under localised loading. Steel Construction, 10 (3), 227-233, 2017.

[42] Uzzaman A, Lim JBP, Nash D, Rhodes J, Young B, Web crippling behaviour of cold-formed steel channel sections with offset web holes subjected to interior-two-flange loading. Thin-Walled Structures, 50, 76–86, 2012.

[43] Uzzaman A, Lim JBP, Nash D, Rhodes J, Young B, Effect of offset web holes on web crippling strength of cold-formed steel channel sections under end-two-flange loading condition. Thin-Walled Structures, 65, 34–48, 2013.

[44] Uzzaman A, Lim JBP, Nash D, Rhodes J, Young B, Cold-formed steel sections with web openings subjected to web crippling under two-flange loading conditions-part II: parametric study and proposed design equations. Thin-Walled Structures, 56, 79–87, 2012.

[45] EN ISO 6892-1:2016. Metallic materials — Tensile testing, Part 1: Method of test at room temperature, London: BSI, 2016.

[46] Cruise R and Gardner L, Residual stress analysis of structural stainless steel sections. Journal of constructional steel research, 64(3), 356-366, 2008.

[47] Sundararajah L, Mahendran M and Poologanathan K, Web crippling studies of SupaCee sections under two flange load cases. Engineering Structures, 153, 582-597, 2017.

[48] Lian Y, Uzzaman A, Lim JBP, Abdelal G, Nash D and Young B, Effect of web holes on web crippling strength of cold-formed steel channel sections under end-one-flange loading condition – part I: tests and finite element analysis. Thin-Walled Structures, 107, 443–452, 2016.

[49] Lian Y, Uzzaman A, Lim JBP, Abdelal G, Nash D and Young B, Effect of web holes on web crippling strength of cold-formed steel channel sections under end-one-flange loading condition – part II: parametric study and proposed design equations. Thin-Walled Structures, 107, 489–501, 2016.

[50] Chen Y, Chen X, Wang C, Experimental and finite element analysis research on cold-formed steel lipped channel beams under web crippling. Thin-Walled Structures, 87, 41–52, 2015.

[51] Uzzaman A, Lim JBP, Nash D, Rhodes J and Young B, Cold-formed steel sections with web openings subjected to web crippling under two-flange loading conditions-part I: tests and finite element analysis. Thin-Walled Structures, 56, 38–48, 2012.